

# Luminescent property modification of $\text{SiO}_x/\text{Al}_2\text{O}_3$ multilayers by annealing and hydrogenation

D A Grachev<sup>1</sup>, A M Legkov<sup>1</sup>, I I Chudin<sup>2</sup> and A V Ershov<sup>1</sup>

<sup>1</sup> Department of Semiconductor Physics and Optoelectronics,  
Lobachevsky University, Nizhny Novgorod 603950, Russia

<sup>2</sup> Research Institute of Physics and Technology,  
Lobachevsky University, Nizhny Novgorod 603950, Russia

E-mail: grachov@phys.unn.ru

**Abstract.** We have studied the composite nanopariodic (3-8 nm)  $\text{SiO}_x/\text{Al}_2\text{O}_3$  structures fabricated by physical deposition from separate sources. The structures annealed in nitrogen atmosphere at 900–1100 °C included Si-NCs that showed intense room-temperature photoluminescence at 1.6 eV. The quantum-confinement peak shift was observed under varying the  $\text{SiO}_x$  layer thickness. Up to fourfold intensity enhancement was observed after hydrogenation of the structures in the range of 400–450 °C for 2 hours.

## 1. Introduction

In recent years there has been a significant growth of interest in the study of silicon nanocrystals (Si-NCs) in various dielectric layers, matrices alternative to silicon oxide [1–4]. We present the results of an optical properties study of the composite dielectric films obtained by high-temperature annealing of nanopariodic  $\text{SiO}_x/\text{Al}_2\text{O}_3$  sandwich structures and containing ordered arrays of Si-NCs. According to the transparency range, alumina is similar to silica but it has a higher refractive index (1.7 vs. 1.5 [5]). Thus, the variation of the dielectric matrix material may be an additional tool to control the effective refractive index of the composites as the active medium for silicon photonics.

Apart from preparing samples, a problem of enhancement of the Si-NCs photoluminescence (PL) intensity by hydrogenation has drawn our attention. The principal possibility of controlling the intensity by passivation of the defect centers [6,7] is fundamentally important in terms of understanding the PL mechanism as well as exciton localization in Si-NCs in particular [8,9].

## 2. Preparation of samples and measurements procedure

The  $\text{SiO}_x/\text{Al}_2\text{O}_3$  multilayer structures with layer thicknesses of 3-8 nm and a number of layers up to 60 were fabricated by physical deposition on silicon substrates (table 1). To obtain ordered arrays of Si-NCs, as described in refs. [10–12], the samples were annealed at 1000 – 1100 °C in a dry nitrogen atmosphere for 2 hours.

Hydrogenation was carried out in an environment of molecular hydrogen (1 atm.) at 400 – 550 °C for 2 hours. Subsequent dehydrogenation was performed in nitrogen atmosphere at temperatures of 600 – 700 °C but for just one hour. Figure 1 as well as table 2 clarifies the details.



**Table 1. Sample description**

| Sample     | Thicknesses<br>of a bilayer (nm\nm) | Number of layers |
|------------|-------------------------------------|------------------|
| $\alpha 1$ | 8\3                                 | 19               |
| $\alpha 2$ | 4\3                                 | 56               |
| $\alpha 3$ | 2\3                                 | 60               |

The stationary PL measurements were carried out at room temperature using a Nanometrics RPM PL Wafer Mapping System in the range of 580–1100 nm, the samples were pumped with the radiation of a Nd:YAG laser at  $\lambda = 532$  nm with a power of 26 mW (a power density of 325 mW/cm<sup>2</sup>). We used a CCD 512-TE detector in tandem with a 570LP filter.

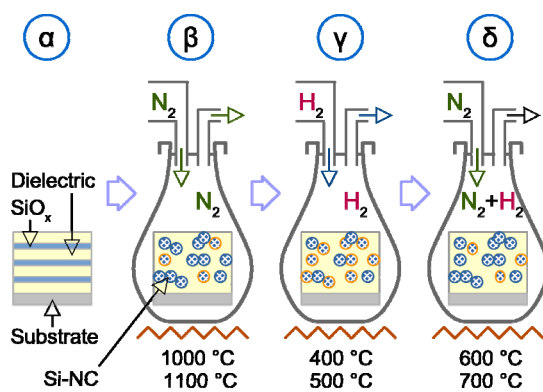


**Figure 1.** Schematic representation of the  $\text{SiO}_x/\text{Al}_2\text{O}_3$  nanostructure modification. Circled letters are keys that symbolize modification steps:  $\alpha$  is forming,  $\beta$  is annealing,  $\gamma$  is hydrogenation,  $\delta$  is dehydrogenation.

The IR-transmission spectra in the range of 400–1400  $\text{cm}^{-1}$  were recorded with a spectrometer (Varian 4100 Excalibur, a spectral resolution of 2  $\text{cm}^{-1}$ ) by the method of multiple signal accumulation.

**Table 2. Treatment parameters**

|                    | Annealing – $\beta$ , 2h |           | Hydrogenation – $\gamma$ , 2h |             |             |             | Dehydrogenation – $\delta$ , 1h |             |             |
|--------------------|--------------------------|-----------|-------------------------------|-------------|-------------|-------------|---------------------------------|-------------|-------------|
| Temperature (°C)   | 1000                     | 1100      | 400                           | 450         | 500         | 550         | 600                             | 650         | 700         |
| Sample designation | $\beta 0$                | $\beta 1$ | $\gamma 40$                   | $\gamma 45$ | $\gamma 50$ | $\gamma 55$ | $\delta 60$                     | $\delta 65$ | $\delta 70$ |

### 3. Experimental results and discussion

#### 3.1. The optical properties of the structures under annealing

Figure 2 shows the typical IR transmittance spectra for sample  $\alpha 1$  annealed at different temperatures. There are a few absorption peaks [13] in the range from 400 to 1400  $\text{cm}^{-1}$ . The 800  $\text{cm}^{-1}$  band associated with ring-like configurations of silicon atoms separated from each other by oxygen atoms is observed when the temperature is not higher than 500 °C. Upon annealing at 600 °C, a broad absorption peak emerges at a frequency of 810  $\text{cm}^{-1}$  corresponding to the bending vibrations of Si-O-Si groups [3,14]. As to the 1050  $\text{cm}^{-1}$  peak associated with the asymmetric vibrations of Si-O-Si groups, it becomes stronger and shifts to higher frequencies. The 435  $\text{cm}^{-1}$  band corresponding to the transverse optical rocking vibrations of Si-O-Si groups in  $\text{SiO}_2$  does likewise. Thus, the absorption bands specific to the Si-O-Si vibration modes in silicon monoxide are transformed into the absorption bands typical of vibration modes of silicon dioxide (e.g.  $2\text{SiO}_x \rightarrow x\text{SiO}_2 + (2-x)\text{Si}$  reaction takes place).

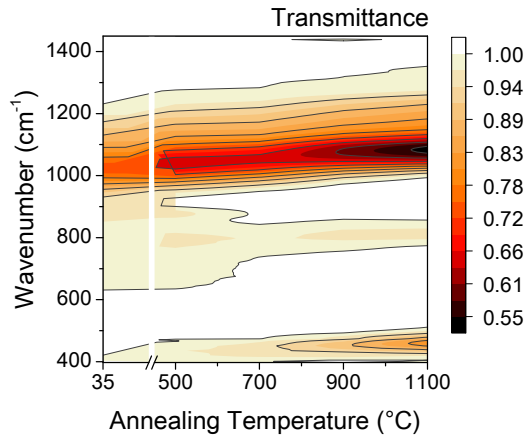


**Figure 2.** FTIR counterplot spectra of the annealed nanostructure  $\alpha 1$  (8nm/3nm).

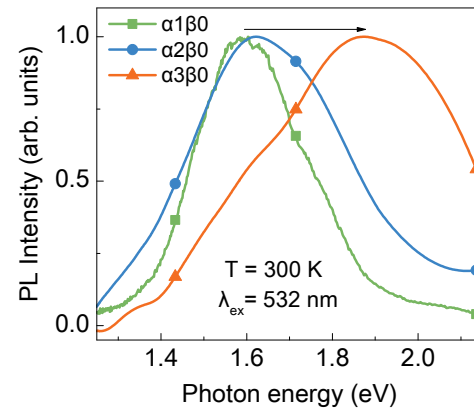


**Figure 3.** Normalized RT PL spectra of the structures annealed at 1000 °C that demonstrate a shift of the Si-NC peak.

The PL spectra are shown in figures 3 and 4. Depending on the temperature, we observe two intensive PL bands. The first one at 1.8 eV appears when the temperature is about 600 °C. We can assume that the band is caused by defects, since its position on the energy scale is constant for all the studied systems. Referring to the discussion of the IR-transmittance results, it can be concluded that a source is the dangling bonds of silicon-oxygen (810  $\text{cm}^{-1}$ ). Aluminium is expected to have a little effect on the oxidation process, since, as well-known, silicon is more electronegative than aluminium.

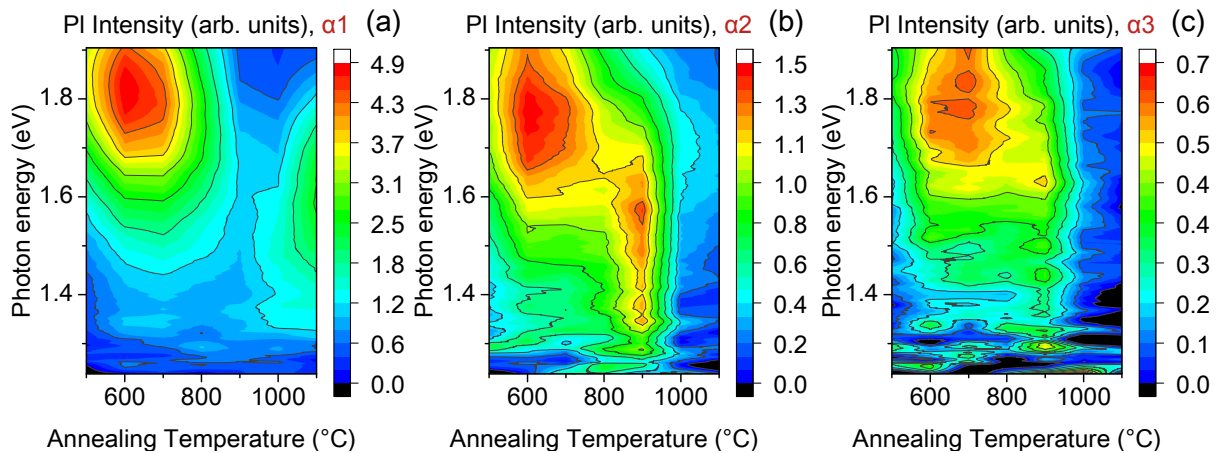


**Figure 4.** RT PL counterplot of the annealed nanostructures: (a)  $\alpha 1$ , (b)  $\alpha 2$ , (c)  $\alpha 3$ .

The second band around 1.6 eV seems to be associated with Si-NCs [6,10,15]. According to the spectra, the preferable temperature for forming is about 900–1100 °C (lower than for  $\text{SiO}_2$  [13]), and it is determined by the thicknesses of the initial  $\text{SiO}_x$  layers. Thus, the thicker the base layer, the higher the annealing temperature is needed. This fact indicates that the 1.6 eV band is related to the diffusion process, and this is a proof that the source is Si-NCs. In order to compare the systems, we considered them at the same annealing temperature of 1000 °C ( $\beta 0$ ). In this case, based on the slight PL shift (figure 3, X-section of the items in figure 4 at 1000 °C is not clear enough) due to the confinement phenomena, there are the samples with different size Si-NCs, wherein the Si-NC size is proportional [10,13] to the thickness of the  $\text{SiO}_x$  layers (table 1).

### 3.2. The optical properties of the structures under hydrogenation and dehydrogenation

Figure 5 shows the typical PL spectra before and after hydrogenation at different temperatures. Annealing the samples at 400–550 °C in the hydrogen atmosphere leads to several-fold enhancement of the PL intensity [16], and here we observe a weak shift of the PL band due to the passivation of the dangling bonds, which is more effective for comparatively large Si-NCs [6]. As the temperature increases, the process comes to naught because of the growth of the hydrogen effusion [17]. Subsequent dehydrogenation of the samples in hydrogen-free environment at temperatures of 600–700 °C leads to a significant decrease of the PL intensity (figure 6) as a result of the hydrogen effusion. This proves the fact that the increase in the PL intensity should be associated with the passivation of the dangling bonds by hydrogen.

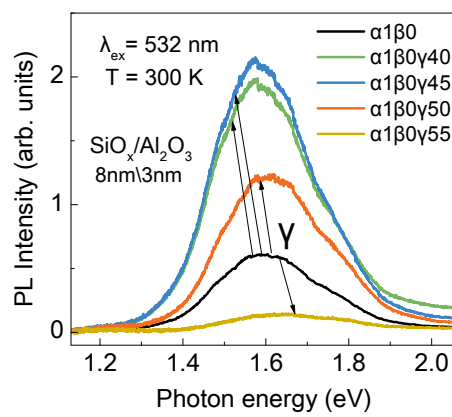


**Figure 5.** RT PL spectra of the  $\alpha 1$  nanostructure (8nm/3nm) under various temperatures of hydrogenation.

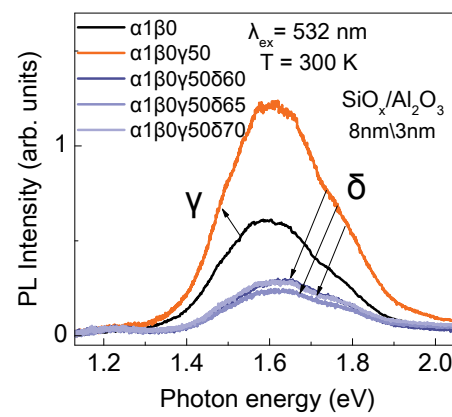


**Figure 6.** RT PL spectra of the  $\alpha 1$  nanostructure (8nm/3nm) under various temperatures of dehydrogenation.

Figure 7 shows the curves of the normalized PL intensity versus the hydrogenation temperature. It is easy to see that the optimal temperature is in the range of 400 – 450 °C. Although sample  $\alpha 1$  (8nm/3nm) shows the highest integrated PL intensity, sample  $\alpha 2$  (4nm/3nm) demonstrates a better enhancement under hydrogenation.

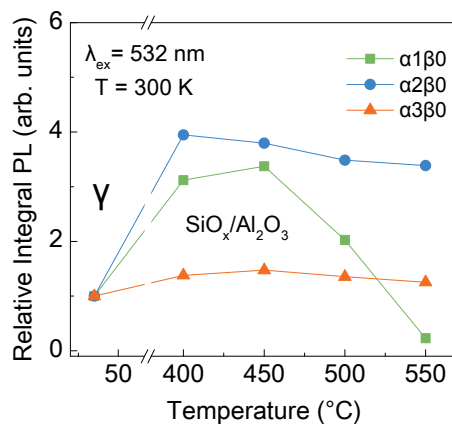


**Figure 7.** Normalized RT PL intensity of the nanostructures under various temperature of hydrogenation.

## 4. Summary

We have studied the composite nanoparodic  $\text{SiO}_x/\text{Al}_2\text{O}_3$  structures fabricated by physical deposition from separate sources. Depending on the  $\text{SiO}_x$  layer thicknesses, the structures included Si-NCs after

annealing in the temperature range of 900 – 1100 °C that is lower than for SiO<sub>x</sub>/SiO<sub>2</sub> counterparts. The structures showed intense room-temperature photoluminescence, the band position of which demonstrated the quantum-confinement phenomena. Under hydrogenation in the range of 400 – 450 °C, the photoluminescence intensity of the samples was enhanced several fold.

The study was partially supported by RFBR (grants #14-02-00119 and #15-02-05086) and by the Ministry of Education and Science of the Russian Federation (state assignment #3.285.2014/K).

## References

- [1] Turishchev S Y, Terekhov V A, Koyuda D A, Pankov K N, Ershov A V, Grachev D A, Mashin A I and Domashevskaya E P 2013 *Semiconductors* **47** 1316–23
- [2] Ershov A V, Pavlov D A, Grachev D A, Bobrov A I, Karabanova I A, Chugrov I A and Tetelbaum D I 2014 *Semiconductors* **48** 42–5
- [3] Mikhaylov A N, Belov A I, Kostyuk A B, Zhavoronkov I Y, Korolev D S, Nezhdanov A V, Ershov A V, Guseinov D V, Gracheva T A, Malygin N D, Demidov E S and Tetelbaum D I 2012 *Phys. Solid State* **54** 368–82
- [4] Grachev D A, Garakhin S A, Belolipetsky A V, Nezhdanov A V and Ershov A V 2016 *J. Phys. Conf. Ser.* **741** 12129
- [5] Palik E D 1998 *Handbook of Optical Constants of Solids II* (Academic Press)
- [6] Garcia C, Garrido B, Pellegrino P, Ferre R, Moreno J A, Morante J R, Pavesi L and Cazzanelli M 2003 *Appl. Phys. Lett.* **82** 1595–7
- [7] Bi L and Feng J Y 2006 *J. Lumin.* **121** 95–101
- [8] Gusev O B, Ershov A V, Grachev D A, Andreev B A and Yablonskiy A N 2014 *J. Exp. Theor. Phys.* **118** 830–7
- [9] Gert A V and Yassievich I N 2015 *Semiconductors* **49** 492–7
- [10] Zacharias M, Heitmann J, Scholz R, Kahler U, Schmidt M and Bläsing J 2002 *Appl. Phys. Lett.* **80** 661
- [11] Turishchev S Y, Terekhov V A, Koyuda D A, Spirin D E, Parinova E V, Nesterov D N, Grachev D A, Karabanova I A, Ershov A V, Mashin A I and Domashevskaya E P 2015 *Semiconductors* **49** 409–13
- [12] Ershov A V, Pavlov D A, Grachev D A, Bobrov A I, Karabanova I A, Chugrov I A and Tetelbaum D I 2014 *Semiconductors* **48** 42–5
- [13] Ershov A V, Chugrov I A, Tetelbaum D I, Mashin A I, Pavlov D A, Nezhdanov A V, Bobrov A I and Grachev D A 2013 *Semiconductors* **47** 481–6
- [14] Tsu D V, Lucovsky G and Davidson B N 1989 *Phys. Rev. B* **40** 1795–805
- [15] Vaccaro L, Spallino L, Zatsepin A F, Buntov E A, Ershov A V, Grachev D A and Cannas M 2015 *Phys. Status Solidi* **252** 600–6
- [16] Li Y, Liang P, Hu Z, Guo S, You Q, Sun J, Xu N and Wu J 2014 *Appl. Surf. Sci.* **300** 178–83
- [17] Kim K-H, Johnson E V. and Roca i Cabarrocas P 2016 *Jpn. J. Appl. Phys.* **55** 72302